Systemic levels of the soluble co-inhibitory and co-stimulatory immune checkpoint molecules in basal cell carcinoma.

Mahlatse C.M. Kgokolo [1], Nonkululeko Z. Malinga [1], Helen C. Steel [2], Pieter W.A. Meyer [2,3], Teresa Smit [4], Ronald Anderson [2], Bernardo L. Rapoport [2,4]

[1]*Department of Dermatology, Faculty of Health Sciences, University of Pretoria and Steve Biko Academic Hospital, Pretoria, South Africa.*

[2]*Department of Immunology, School of Medicine, Faculty of Health Sciences, University of Pretoria, Pretoria, South Africa.*

[3]*Tshwane Academic Division of the National Health Laboratory Service, Pretoria, South Africa.*

[4]*The Medical Oncology Centre of Rosebank, Saxonwold, Johannesburg, South Africa.*

Background

- Basal cell carcinoma (BCC) is the most common malignancy, comprising about 75 % of all cases of skin cancer, and the incidence is rising[1,2].
- BCC rarely metastasizes and the mortality rate is low; however, the disease is associated with substantial morbidity[3].
- The hedgehog intracellular signalling pathway regulates cell growth, and aberrant activation of this pathway leads to BCC development[3]. The hedgehog inhibitors vismodegib and sonidegib are currently approved for systemic therapy of BCC in Europe[3,4,5].
- Hedgehog-dependent tumors are characterized by increased infiltration or the presence of suppressive immune cells, such as M2-like tumor-associated macrophages (M2-TAMs), myeloid-derived suppressor cells (MDSCs), regulatory T (Treg) cells, and cancer-associated fibroblasts (CAF)[6-10].
- BCC is associated with increased numbers of regulatory cells (Tregs) and a CAF-induced immunosuppressive microenvironment[11-14].
- Checkpoint proteins are critical for maintaining self-tolerance and modulating the immune responses of effector cells in normal tissues to minimize tissue damage. These proteins also modulate the immune infiltrates in the tumor microenvironment (TME). Cancer cells exploit the up-regulation or down-regulation of these proteins to evade the anti-tumor immune response[15,16].
- Soluble forms of immune checkpoint molecules (ICMs) have recently been identified and can be measured in human plasma; however, their biological and clinical significance remains essentially unknown[17,18]. Co-inhibitory immune checkpoint proteins are primarily involved in promoting inhibitory cell-cell interactions in adaptive immunity, especially tumor immunity.
- The soluble cell-free variants of these molecules are detectable in the circulation of cancer patients where they retain immunosuppressive activity.
- Little is known about the systemic levels of these soluble co-inhibitory and co-stimulatory immune checkpoints in patients with various subtypes of basal cell carcinoma (BCC), which is the most invasive and treatment-resistant type of this most commonly occurring malignancy.
- Our previous research found significantly elevated levels of PD-1, PDL-1, CTLA-4, TIM-3, and LAG-3 in BCC patients and the current study was undertaken to investigate 16 ICM proteins as well as RANTES, FAP, TGF-β1 and arginase.

Methods

Aim

- The study population consisted of a total of 40 South African patients (12F:28M; mean age ±SD: 69.1 ± 11.1 years) with advanced BCC attending the Dermatology Screening Clinic at Steve Biko Academic Hospital, Pretoria, South Africa.
- The cohort was compared a group of control patients (n=20).
- The circulating levels of 17 immune checkpoint-related proteins panel (B- and T-lymphocyte attenuator (BTLA), Glucocorticoid-Induced TNFR-Related protein (GITR), GITR-ligand (GITRL), Herpes Virus Entry Mediator (HVEM), Lymphocyte activation gene-3 (LAG-3), PD-1, PD-L1, PD-L2, T cell immunoglobulin-3 (TIM-3), CD27, CD28, CD80, CD86, CD40, ICOS, TLR-2, and CTLA-4) were profiled in advanced BCC patients (patient characteristics are summarized in table 1) and compared to those of 20 healthy controls.
- Additionally, we measured plasma levels of arginase, CCL5 (RANTES), TGF-β1 and fibroblast associated protein (FAP).
- A combination of multiplex bead array, laser nephelometry and ELISA technologies were used.
- Ethics approval was granted by the Research Ethics Committee of the Faculty of Health Sciences,

Statistical Analysis

- The primary hypothesis was that that there was a significant difference in the plasma levels of soluble co-inhibitory immune checkpoints between BCC patients and healthy controls.
- Descriptive statistics were used to tabulate patient characteristics.
- The Mann Whitney U-test was used to compare levels of the various test biomarkers between BCC patients and healthy controls.
- The area under the ROC curve (AUC) was used as a measure of discriminatory ability for the biomarkers. The Youden index, a summary measure of the ROC curve, was used as an agnostic method for choosing an optimal cut-off value on the biomarker value to illustrate potential clinical usefulness.
- A correlation matrix report was used to identify correlations between variables (or subsets of variables) within the subset, using Spearman *p*-values to define significance.
- A *p*-value of less than .05 was considered statistically significant.
- NCSS 2021 software for Windows (USA) was used for statistical analyses.

Results

Table 1. Numbers of patients with distinct clinical types of basal cell carcinoma (BCC).

Clinical subtype of BCC	
Adenoid	(n=1)*
Basosquamous	(n=3)
Infiltrating	(n=22)
Infiltrating with squamous differentiation	(n=4)
Keratotic	(n=1)
Micronodular	(n=2)
Nodular	(n=5)
Pigmented	(n=1)^
Superficial	(n=1)^

Table 2. Numbers of patients with basal cell carcinomas at distinct anatomical sites.

Anatomical site	
Cheek	(n=3)^ ^
Chest	(n=2)
Ear	(n=4)
Forearm	(n=4)
Forehead	(n=2)
Lower limb	(n=5)
Neck	(n=2)
Nose	(n=13)^
Shoulder	(n=1)
Temple	(n=2)
Upper anterior chest	(n=2)

**Numbers of patients are shown in parenthesis; ^African patient; ^Asian patient*

Table 3. Comparison of the systemic concentrations of co-inhibitory, and co-stimulatory soluble immune checkpoint proteins in patients with advanced basal cell carcinoma and control participants.

	ICM		BCC (n=40) Median pg/ml (95%CI)	Controls (n=20) Median pg/ml (95%CI)	*p* value
Co-stimulatory	CD27	UP	3360,665 (2260,64 - 4970,73)	1410,54 (1259,16 - 2172,74)	0.0002
	CD28	UP	17047,05 (8487,16 - 30677,1)	11314,17 (7236,45 - 14883,36)	0.2523
	CD40	UP	1308,5 (968,17 - 1779,77)	1222,255 (769,43 - 1349,26)	0.4148
	ICOS	UP	15359,79 (7591,11 - 20308,75)	12902,86 (7980,59 - 15316,53)	0.3428
	GITR	UP	1217,4 (664,31 - 1795,54)	698,205 (228,01 - 1222,24)	0.0538
	GITRL	UP	2527,32 (1470,48 - 3099,4)	2107,325 (1784,1 - 2724,34)	0.3799
	CD86	UP	2215,865 (793,93 - 3292,87)	1636,65 (781,54 - 2144,3)	0.2427
	CD80	UP	1450,26 (803,6 - 2161,26)	1212,29 (781,71 - 1590,1)	0.3428
Co-inhibitory	PD-1	UP	10978,21 (5714,49 - 14351,17)	2524,69 (1832,95 - 3038,34)	0.0000
	PD-L1	UP	1740,25 (773,982 - 1980,649)	228,67 (139,51 - 274,66)	0.0000
	PD-L2	UP	14705,27 (13102,68 - 16375,87)	12008,07 (10670,4 - 14023,9)	0.0011
	CTLA-4	UP	744,92 (422,08 - 1129,16)	126,49 (56,24 - 241,25)	0.0000
	TIM-3	UP	7519,74 (6619,886 - 8157,926)	12008,07 (10670,4 - 14023,9)	0.0000
	LAG-3	UP	386288,90 (243248,3 - 540480,6)	11106,96 (6595,67 - 15093,31)	0.0000
	BTLA	DOWN	12284,97 (8754,07 - 19151,59)	25439,74 (17274,69 - 32427,56)	0.0061
Dual	TLR-2	UP	17696,28 (10473,49 - 24211,18)	15731,88 (12262,72 - 19913,19)	0.6437
	HVEM	UP	2052,45 (1894,5 - 2317,55)	1299,11 (1263,46 - 1458,94)	0.0000
Other	Arginase		25,52 (25,52 - 29,8505)	25,52 (25,52 - 72,15)	0.2897
	RANTES	UP	131,46 (97,25 - 174,9144)	90,83 (70,78 - 148,71)	0.2097
	TGF-β1	UP	7,54 (4,549417 - 10,79543)	5,85 (4,18 - 6,83)	0.1469
	FAP	UP	115,67 (94,02 - 130,19)	109,04 (70,83 - 127,33)	0.2425

Table 4. ROC curve cut-off values (using Youden Index) and AUC (95% CI) for immune checkpoint molecules.

	Soluble Immune Checkpoint Molecule (pg/mL)	AUC (CI 95%)	Cut-off point (pg/mL)	Sensitivity (TPR) %	Specificity (TNR) %	p ≤
Co-stimulatory	CD27	0,204	≤ 2989,38	40	100	1,0000
	CD28	0,591	≥ 20005,17	48	75	0,1066
	CD40	0,565	≥ 1701,52	40	90	0,1971
	ICOS	0,576	≥ 17225,11	48	85	0,1505
	GITR	0,654	≥ 2001,53	33	100	0,0158
	GITRL	0,570	≥ 4107,31	33	100	0,1692
	CD86	0,593	≥ 2609,66	45	90	0,0998
	CD80	0,576	≥ 2200,90	33	100	0,1491
Co-inhibitory	PD-1	0,874	≥ 4849,52	73	95	0,0000
	PD-L1	0,926	≥ 404,54	89	95	0,0000
	PD-L2	0,761	≥ 11788,96	90	50	0,0000
	CTLA-4	0,689	≥ 292,80	73	95	0,0000
	TIM-3	0,996	≥ 3774,69	98	100	0,0000
	LAG-3	1,000	≥ 33502,53	100	100	0,0000
	BTLA	0,281	≥ 15585,46	43	20	0,9991
Dual	TLR-2	0,537	≥ 22486,86	40	90	0,3081
	HVEM	0,916	≥ 1524,59	90	90	0,0000
Other	Arginase	0,420	≥ 36,62	23	55	0,8537
	RANTES	0,600	≥ 198,72	33	95	0,0861
	TGF-β1	0,616	≥ 8,21	43	100	0,0042
	FAP	0,593	≥ 141,20	33	100	0,1047

Figure 1. Comparison of plasma levels of inhibitory immune checkpoints between BCC patients and healthy controls.

Figure 1a: PD-1 levels of BCC patients vs healthy controls (*p*<0.0000)

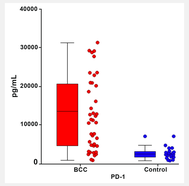

Figure 1b: PD-L1 levels of BCC patients vs healthy controls (*p*<0.0000)

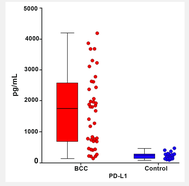

Figure 1c: LAG-3 levels of BCC patients vs healthy controls (*p*<0.0000)

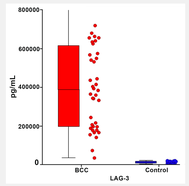

Figure 1d: CTLA-4 levels of BCC patients vs healthy controls (*p*<0.0000)

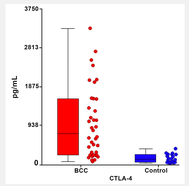

Figure 1e: TIM-3 levels of BCC patients vs healthy controls (*p*<0.0000)

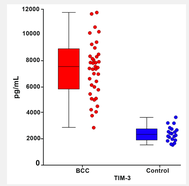

Figure 2. ROC curves of inhibitory immune checkpoints.

Figure 2a. ROC curve of PD-1 with AUC=0.87, confidence interval (95%): 73-95, *p*<0.0000

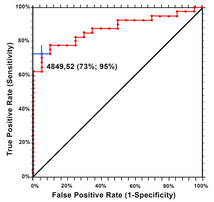

Figure 2b. ROC curve of PD-L1 with AUC=0.93, confidence interval (95%): 89-95, *p*<0.0000

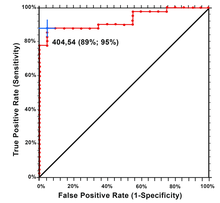

Figure 2c. ROC curve of LAG-3 with AUC=1.00, *p*<0.0000

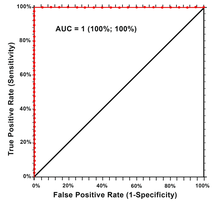

Figure 2d. ROC curve of CTLA-4 with AUC=0.89, confidence interval (95%): 73-95, *p*<0.0000

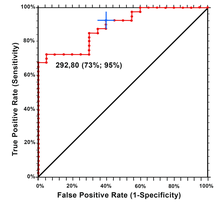

Figure 2e. ROC curve of TIM-3 with A UC=0.99, confidence interval (95%): 98-100, *p*<0.0000

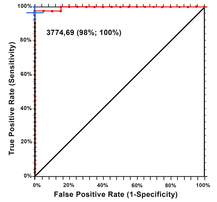

Figure 3. Correlation plots of significant correlations between TGF-β1 and other ICM plasma levels in BCC patients.

Figure 3a: Correlation of TGF-β1 and PD-1 in BCC patients (*p*<0.0000, Spearman 0.75)

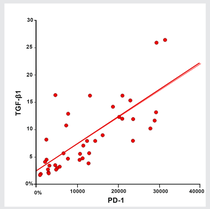

Figure 3b: Correlation of TGF-β1 and LAG-3 in BCC patients (p<0.0000, Spearman 0.80)

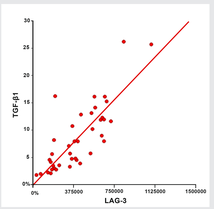

Figure 3c: Correlation of TGF-β1 and PD-L1 in BCC patients (*p*<0.0000, Spearman 0.76)

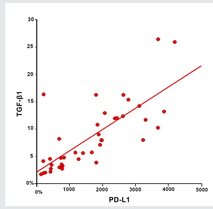

Figure 3d: Correlation of TGF-β1 and GIRTL in BCC patients (*p*<0.0000, Spearman 0.77)

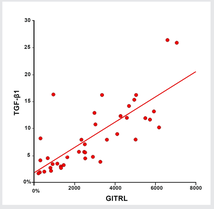

Figure 3e: Correlation of TGF-β1 and GITR in BCC patients (*p*<0.0000, Spearman 0.81)

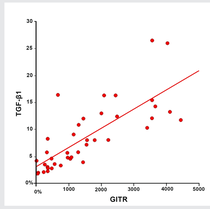

Figure 3. Clustered Heat Map.

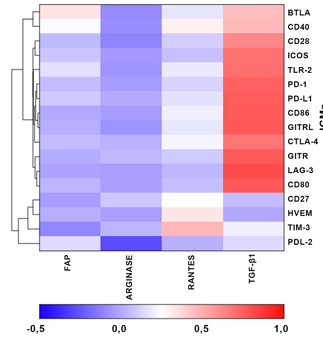

Conclusions

- This seemingly novel finding not only identifies the existence of significant systemic immunosuppression in BCC, but also underscores the therapeutic promise of immune checkpoint targeted therapy.
- The study demonstrates the potential of these proteins to serve as prognostic/predictive biomarkers in BCC.
- The therapeutic potential of dual targeting of PD-1 and TIM-3 or LAG-3 in this condition, as well as treatment with checkpoint inhibitors early in the course of the disease, is warranted.
- We found plasma levels of TGF-β1, as a biomarker for Tregs, showing significant positive correlations with GITR, GITRL, LAG-3 PD-1, PD-L1, CD80, and CD86.
- There were no correlations found between any of the ICMs and FAP, arginase or RANTES respectively.

References

1. Verkouteren, J.A.C.; Ramdas, K.H.R.;Wakkee, M.; Nijsten, T Epidemiology of basal cell carcinoma: scholarly review. Br J Dermatol. 2017 Aug;177(2):359-372. doi: 10.1111/bjd.15321. Epub 2017 Feb 20. PMID: 28220485
2. Heidi-Philipp M, Frischhut N, Hölweger N, Schmuth M, Nguyen VA. Known and new facts on basal cell carcinoma. J Dtsch Dermatol Ges. 2021 Jul;19(7):1021-1041. doi: 10.1111/ddg.14580. PMID: 34288482
3. Fania L, Didona D, Morese R, Campana I, Coco V, Di Pietro FR, Ricci F, Pallotta S, Candi E, Abeni D, Dellambra E. Basal Cell Carcinoma: From Pathophysiology to Novel Therapeutic Approaches. Biomedicines. 2020 Oct 23;8(11):449. doi: 10.3390/biomedicines8110449. PMID: 33113965
4. Kim DP, Kus KJB, Ruiz E. Basal Cell Carcinoma Review. Hematol Oncol Clin North Am. 2019 Feb;33(1):13-24. doi: 10.1016/j.hoc.2018.09.004. PMID: 30497670
5. Tanese K. Diagnosis and Management of Basal Cell Carcinoma. Curr Treat Options Oncol. 2019 Feb 11;20(2):13. doi: 10.1007/s11864-019-0610-0. PMID: 30741348 Review.
6. Hedgehog signaling promotes tumor-associated macrophage polarization to suppress intratumoral CD8+ T cell recruitment. J Clin Invest. 2019 Dec 2;129(12):5151-5162. doi: 10.1172/JCI128644. PMID: 31638600
7. Hinshaw DC, Hanna A, Lama-Sherpa T, Metge B, Kammerud SC, Benavides GA, Kumar A, Alsheikh HA, Mota M, Chen D, Ballinger SW, Rathmell JC, Ponnazhagan S, Darley-Usmar V, Samant RS, Shevde LA. Hedgehog Signaling Regulates Metabolism and Polarization of Mammary Tumor-Associated Macrophages. Cancer Res. 2021 Nov 1;81(21):5425-5437. doi: 10.1158/0008-5472.CAN-20-1723. Epub 2021 Jul 21. PMID: 34289986.
8. Xie J. The hedgehog's trick for escaping immunosurveillance: The molecular mechanisms driving myeloid-derived suppressor cell recruitment in hedgehog signaling-dependent tumors. Oncoimmunology. 2014 Jun 5;3:e29180. doi: 10.4161/onci.29180. eCollection 2014. PMID: 25054089
9. Grund-Gröschke S, Stockmaier G, Aberger F. Hedgehog/GLI signaling in tumor immunity - new therapeutic opportunities and clinical implications. Cell Commun Signal. 2019 Dec 26;17(1):172. doi: 10.1186/s12964-019-0459-7. PMID: 31878932
10. Valenti G, Quinn HM, Heynen GJJE, Lan L, Holland JD, Vogel R, Wulf-Goldenberg A, Birchmeier W. Cancer Stem Cells Regulate Cancer-Associated Fibroblasts via Activation of Hedgehog Signaling in Mammary Gland Tumors. Cancer Res. 2017 Apr 15;77(8):2134-2147. doi: 10.1158/0008-5472.CAN-15-3490. Epub 2017 Feb 15. PMID: 28202523
11. Omland SH, Nielsen PS, Gjerdrum LM, Gniadecki R. Immunosuppressive Environment in Basal Cell Carcinoma: The Role of Regulatory T Cells. Acta Derm Venereol. 2016 Nov 2;96(7):917-921. doi: 10.2340/00015555-2440. PMID: 27117439
12. Omland SH, Hamrouni A, Gniadecki R. High diversity of the T-cell receptor repertoire of tumor-infiltrating lymphocytes in basal cell carcinoma. Exp Dermatol. 2017 May;26(5):454-456. doi: 10.1111/exd.13240. Epub 2017 Jan 19. PMID: 27714856
13. Omland SH, Wettergren EE, Mollerup S, Asplund M, Mourier T, Hansen AJ, Gniadecki R. Cancer associated fibroblasts (CAFs) are activated in cutaneous basal cell carcinoma and in the peritumoural skin. BMC Cancer. 2017 Oct 7;17(1):675. doi: 10.1186/s12885-017-3663-0. PMID: 28987144
14. Omland SH. Local immune response in cutaneous basal cell carcinoma. Dan Med J. 2017 Oct;64(10):B5412. PMID: 28975891
15. Zhang Y, Zheng J. Functions of Immune Checkpoint Molecules Beyond Immune Evasion. Adv Exp Med Biol. 2020;1248:201-226. doi: 10.1007/978-981-15-3266-5_9. PMID: 32185712
16. Tu L, Guan R, Yang H, Zhou Y, Hong W, Ma L, Zhao G, Yu M. Assessment of the expression of the immune checkpoint molecules PD-1, CTLA4, TIM-3 and LAG-3 across different cancers in relation to treatment response, tumor-infiltrating immune cells and survival. Int J Cancer. 2020 Jul 15;147(2):423-439. doi: 10.1002/ijc.32785. Epub 2019 Dec 2. PMID: 31721169
17. Gu D, Ao X, Yang Y, Chen Z, Xu X. Soluble immune checkpoints in cancer: production, function and biological significance. J Immunother Cancer. 2018 Nov 27;6(1):132. doi: 10.1186/s40425-018-0449-0. PMID: 30482248
18. Chakrabarti R, Kapse B, Mukherjee G. Soluble immune checkpoint molecules: Serum markers for cancer diagnosis and prognosis. Cancer Rep (Hoboken). 2019 Aug;2(4):e1160. doi: 10.1002/cnr2.1160. Epub 2019 Feb 7.PMID: 32721130
19. Malinga NZ, Siwele SC, Steel HC, Kwofie LLI, Meyer PWA, Smit T, Anderson R, Rapoport BL, Kgokolo MCM. Systemic levels of the soluble co-inhibitory immune checkpoints, CTLA-4, LAG-3, PD-1/PD-L1 and TIM-3 are markedly increased in basal cell carcinoma. Transl Oncol. 2022 May;19:101384. doi: 10.1016/j.tranon.2022.101384. Epub 2022 Mar 4. PMID: 35255355

2022 SITC 37th Annual Meeting - November 8 - 12, 2022; Boston, Massachusetts

Corresponding author: bernardo.rapoport@up.ac.za